Robotica (2002) volume 20, pp. 607–613. © 2002 Cambridge University Press
DOI: 10.1017/S0263574702004423 Printed in the United Kingdom

Effect of base compliance on the dynamic stability of mobile manipulators

R. F. Abo-Shanab and N. Sepehri*

Department of Mechanical and Industrial Engineering, The University of Manitoba, Winnipeg, Manitoba (Canada) R3T-5V6

(Received in Final Form: July 22, 2002)

SUMMARY

This paper extends the model developed previously by the authors,[1] for studying dynamic stability of mobile manipulators. The extended model not only takes into account the dynamics of the base that can potentially rock back-and-forth, but also accounts for the flexibility of the contact between the base and the ground. A novel method of virtual links is used to reformulate the problem of modeling the non-fixed base manipulator in terms of a fixed-base manipulator with one degree of freedom joints. The resulting model is then used to simulate planar movements of a Caterpillar excavator-based log-loader. The results clearly demonstrate the relationship between movement of the implement and the stability of the machine. The flexible contact between the base and the ground is also shown to influence the stability. The results are also compared with those obtained by the previous model, which assumed rigid contact between the base and the ground. It is demonstrated that the assumption of rigid contact tends to overestimate the stability. Consequently, flexibility in the contact between the base and the ground must be considered to more accurately predict the stability of mobile manipulators.

1. INTRODUCTION

The development of automated systems for the operation of heavy-duty manipulator-like machines, such as log-loaders, has recently received much attention. The environments in which these machines operate are unstructured and potentially hazardous. The operator must remain alert, at all time, in order to accomplish the work efficiently and, at the same time, protect his/her safety and that of others. Current research effort has been to develop means for converting these machines into teleoperated control systems.[2,3] One issue in the computer control of such machines, however, is the ability to maintain stability. A heavy-duty mobile manipulator while carrying a load, experiencing a force, or operating on uneven terrain needs to maintain its balance.

Early work on stability of mobile vehicles was only concerned with the static stability and gait generation of slow moving legged machines. The most comprehensive method belongs to Messuri and Klein[4] who introduced a measure of stability termed energy stability margin. This method, however, could only deal with cases where the only destabilizing load is due to the gravitational force. In a moving-base manipulator a large portion of destabilizing forces and moments could be due to the inertial or external loads arising from maneuvering the end-effector. Nagy et al.[5] extended the energy stability method to take into account the effect of known walker terrain compliance on the stability of the walker. The method is still confined to the stability analysis of vehicles that are subject to only weight forces. Dubowsky and Vance[6] proposed a time optimal motion planning strategy for manipulators that are mounted on mobile platforms. The goal was to allow the manipulators to perform tasks quickly without generating dynamic forces and moments that cause the system to overturn. The method, however, did not attempt to study the tip-over case or to develop a measure of stability. Sugano et al.[7] and Huang et al.[8–10] employed the ZMP (Zero Moment Point) concept to construct a quantitative criterion for manipulators mounted on a vehicle. In their work, the manipulator, including the vehicle and the payload, was considered to be a system of particles moving on only rigid horizontal floors. ZMP concept is a moment-based approach and therefore does not include the effect of the walking height in the stability analysis. Papadopoulos and Rey[11,12] proposed a Force-Angle measure of tip-over stability margin. The Force-Angle stability measure has a simple graphical interpretation and is easy to compute, it, however, does not give any information about the state of base, i.e. whether the base is going to tipover completely or just rock back-and-forth. Iagnemma et al.[13] introduced a kinematic reconfiguration method to enhance system's tip-over stability. The method was built upon the Force-Angle measure method and was intended for quasi-static systems. Ghasempoor and Sepehri[14] extended the energy stability method by Messuri and Klein[4] to quantitatively reflect the effect of forces and moments arising from the manipulation of the implement. The significance of this extension is that it can be used as an off-line tool to provide the designers with an inexpensive and fast method of maintaining the stability of mobile manipulators. The extension, however, does not predict how the base responds to the movement of manipulator links. Recently, Abo-Shanab and Sepehri[1] developed, for the first time, a tipping-over model of mobile manipulators. The model takes into account the dynamics of the base that can rock back-and-forth and includes the impact between the base and the ground. Although the model is capable of producing detailed response of the manipulator including the movement of the base, it relies on the assumption of rigid contact between the base

* Corresponding author, E-mail: nariman@cc.umanitoba.ca

and the ground. This assumption is not realistic. It also results in a non-smooth mathematical model. Dealing with equations of motion for non-smooth systems is more complicated than solving those of smooth systems, since the classical solution theories to ordinary differential equations require vector field to be at least Lipschitz-continuous[15] and non-smooth systems fail this requirement. Thus, Filippov's solution theory[16,17] must be used first, to ensure the existence, continuation, and uniqueness of the solution. This is not easy especially for systems with more than one discontinuity surface, which is the case in their study.

In this paper, we improve the model developed previously,[1] to include the flexibility of the contact between the base and the ground. Inclusion of the flexibility, which is due to the suspension and the tires, results in a more realistic model of the entire system. The approach taken is to first consider the contact between the base and the ground as a multidegree of freedom joint. Next, the novel method of virtual links is employed to cast the resulting problem into a fixed base serial link manipulator with single degree of freedom at each joint. This process further facilitates the derivation of the final dynamic equations. The model is applied to a Caterpillar log-loader machine. These machines incorporate many aspects of typical robotic systems and are the basis for most heavy-duty hydraulic machines. Thus, the analysis and development reported in this paper can be applied to other similar mobile robotic systems or heavy-duty mobile manipulators.

The organization of this paper is as follows. Section 2 describes the method of virtual links. Modelling of the system including the contact flexibility is discussed in Section 3. Section 4 presents the simulation results pertaining the application of the model to a Caterpillar log-loader. Conclusions are given in Section 5.

2. METHOD OF VIRTUAL LINKS

Consider an n-link serial manipulator with $(n+m)$ degrees of freedom. This means that some of the manipulator joints have more then one degree of freedom. To model the manipulator, m virtual links, each with one degree of freedom are added. The original n-link system now becomes an $(n+m)$-link system. Vector $\mathbf{q} = \{q_1, q_2, \ldots, q_{n+m}\}^T$ denotes the generalized coordinates and $\tau = \{\tau_1, \tau_2, \ldots, \tau_{m+n}\}^T$ is the generalized force vector for the new system. The dynamic equations are then derived using Lagrange-Euler (LE) method in the augmented state space.[18,19]

$$\tilde{\mathbf{M}}(\mathbf{q})\ddot{\mathbf{q}} + \tilde{\mathbf{C}}(\mathbf{q}, \dot{\mathbf{q}}) + \tilde{\mathbf{G}}(\mathbf{q}) = \tau \qquad (1)$$

where $\tilde{\mathbf{M}}(\mathbf{q})$ is the symmetric, positive definite inertial accelerationrelated matrix, $\tilde{\mathbf{C}}(\mathbf{q}, \dot{\mathbf{q}})$ is the vector of centripetal and Coriolis torques and $\tilde{\mathbf{G}}(\mathbf{q})$ is the vector of gravitational torques. To obtain the final equations for the original system, all the kinematic and dynamic parameters of the virtual links, such as the masses, moments of inertia or lengths, are set to zero. The final equation for the original multi-link system is then:

$$\mathbf{M}(\mathbf{q})\ddot{\mathbf{q}} + \mathbf{C}(\mathbf{q}, \dot{\mathbf{q}}) + \mathbf{G}(\mathbf{q}) = \tau \qquad (2)$$

where $\mathbf{M}(\mathbf{q})$, $\mathbf{C}(\mathbf{q}, \dot{\mathbf{q}})$, and $\mathbf{G}(\mathbf{q})$ are simplified forms of $\tilde{\mathbf{M}}(\mathbf{q})$, $\tilde{\mathbf{C}}(\mathbf{q}, \dot{\mathbf{q}})$, and $\tilde{\mathbf{G}}(\mathbf{q})$, respectively, since the dynamic and kinematic parameters of the virtual links are set to zero. The detailed description of method with many illustrative examples is given in reference [20].

3. DEVELOPMENT OF THE MODEL

The schematic of a planar mobile manipulator is shown in Figure 1. The base is considered as a rigid body, resting on two wheels that are longitudinally aligned and are modelled using the half car representation with Kelvin-Voigt spring damping system.[21] The system damping is viscous, below the critical value and invariant with respect to changes of the kinematics configuration. In the present model, the base is considered to undergo a heave and a pitch motion. With reference to Figure 1, the manipulator is characterized to operate within two distinct phases:

Phase 1: The base is either resting on both edges $\bar{\mathbf{A}}$ and $\bar{\mathbf{B}}$ or turning over the rear edge $\bar{\mathbf{A}}$. In this phase, the base remains in contact with the ground on edge $\bar{\mathbf{A}}$, at all-time. Thus, in order to model the system, the connection between the point $\bar{\mathbf{A}}$ on the ground and point **A** located on the base, is modelled as a three degree of freedom joint subject to a suspension force F_{susp1} (see Figure 2a). Two virtual links with prismatic joints are therefore added to represent the horizontal and the vertical motions (q_1 and q_2) at this point. Point **B** is subject to force F_{susp2} originated from the suspension between $\bar{\mathbf{B}}$ and **B**. The mobile robot is then considered as a 5-link serial manipulator subject to two external forces F_{susp1} and F_{susp2}.

Phase 2: The base is either resting on both edges $\bar{\mathbf{A}}$ and $\bar{\mathbf{B}}$ or turning over the front edge $\bar{\mathbf{B}}$. In this phase, the base remains in contact with the ground on edge $\bar{\mathbf{B}}$, at all-time. As in the first phase, the connection between the point $\bar{\mathbf{B}}$ on the ground and point **B** located on the base is modelled as a three degree of freedom joint subject to suspension force F_{susp2} (see Figure 2b). Two virtual links with prismatic joints are therefore added to represent the horizontal and the vertical motions (q_1 and q_2) at this point. Point **A** is subject to suspension force F_{susp1}.

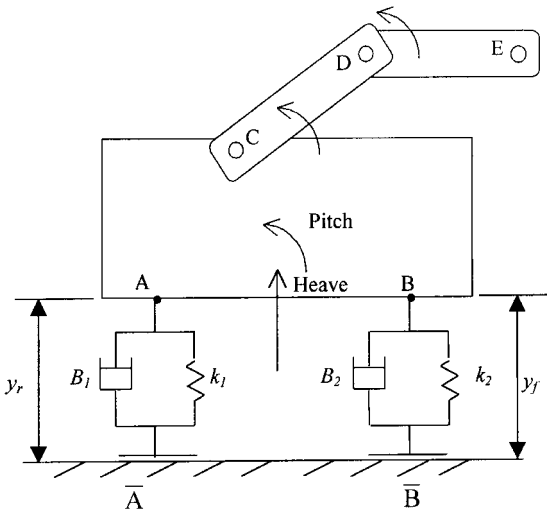

Fig. 1. Schematic of a planar mobile manipulator.

https://doi.org/10.1017/S0263574702004423 Published online by Cambridge University Press

Switching between the two phases is based on calculating the height of the rear and front edges above the ground, i.e. y_r and y_f in Figure 1. As far as y_r is less then the undeformed length of the spring, x_0, the first phase is considered. Once y_r becomes greater than x_0 the second phase is applied.

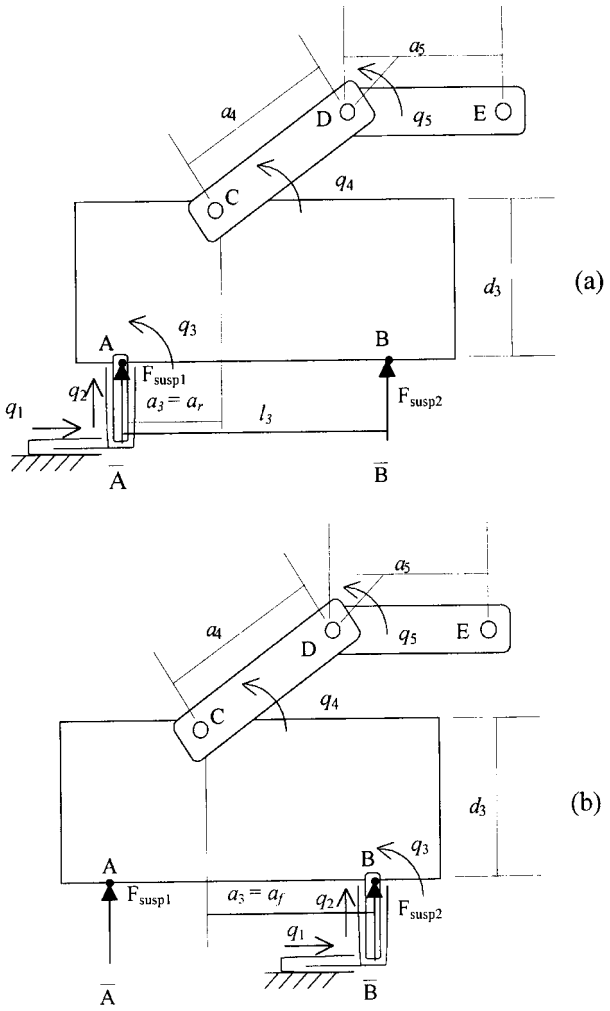

Fig. 2. Schematics of the mobile manipulator including the virtual links.

Figure 3 shows the Denavit-Hartenberg (D-H) coordinate systems applied to both phases. Note that $a_3 = a_r$ when modelling the first phase and $a_3 = -a_f$ for modelling the second phase.

Utilizing the D-H coordinates as described in Figure 3, the dynamic equations describing both phases are then derived as follows:[20]

$$\tau = \mathbf{M}(\mathbf{q})\,\ddot{\mathbf{q}} + \mathbf{C}(\mathbf{q}, \dot{\mathbf{q}}) + \mathbf{G}(\mathbf{q}) + \tau_{susp} \tag{3}$$

where $\mathbf{q} = \{q_1, q_2, \ldots, q_5\}^T$, $\dot{\mathbf{q}}$ and $\ddot{\mathbf{q}}$ are vectors of the joint variables, velocities and accelerations, $\tau(t) = \{\tau_1, \tau_2, \ldots, \tau_5\}^T$ is the generalized force vector applied at joints $i = 1, 2, \ldots, 5$, and $\tau_{susp} = \{\tau_{susp1}, \tau_{susp2}, \tau_{susp3}, \tau_{susp4}, \tau_{susp5}\}^T$ is the external force vector due to suspension forces F_{susp1} and F_{susp2}.

The elements of the 5×5 inertial acceleration-related symmetric matrix, $\mathbf{M}(\mathbf{q})$, are derived using the following relations:

$$\begin{aligned} M_{ij} &= Trace\left\{\Delta_i \left[\sum_{p=j}^{5} \mathbf{T}_p\, \mathbf{J}_p\, \mathbf{T}_p^T\right] \Delta_j^T\right\} \quad (j \geq i) \\ M_{ji} &= M_{ij} \qquad\qquad\qquad\qquad\quad (i < j) \end{aligned} \tag{4}$$

The elements of the Coriolis and centrifugal force vector $\mathbf{C}(\mathbf{q}, \dot{\mathbf{q}}) = \{c_1, c_2, \ldots, c_5\}^T$ are determined as follows:

$$c_i = \sum_{j=1}^{5} \sum_{i=1}^{5} c_{ijk}\, \dot{q}_j\, \dot{q}_k$$

where

$$\begin{aligned} c_{ijk} &= Trace\left\{\Delta_i \left[\sum_{p=j}^{5} \mathbf{T}_p\, \mathbf{J}_p\, \mathbf{T}_p^T\right] \Delta_j^T \Delta_k^T\right\} \quad (j \leq i, j \leq k) \\ c_{ikj} &= c_{ijk} \\ c_{kji} &= -c_{ijk} \qquad\qquad\qquad\qquad\quad (j < i, j < k) \end{aligned} \tag{5}$$

The elements of the gravitational force vector $\mathbf{G}(\mathbf{q}) = \{G_1, G_2, \ldots, G_5\}^T$ are:

$$G_i = -(\mathbf{g}^T; 0)\, \Delta_i \left[\sum_{p=i}^{5} m_p\, \mathbf{T}_p\, (\mathbf{r}_p^p; 1)\right] \tag{6}$$

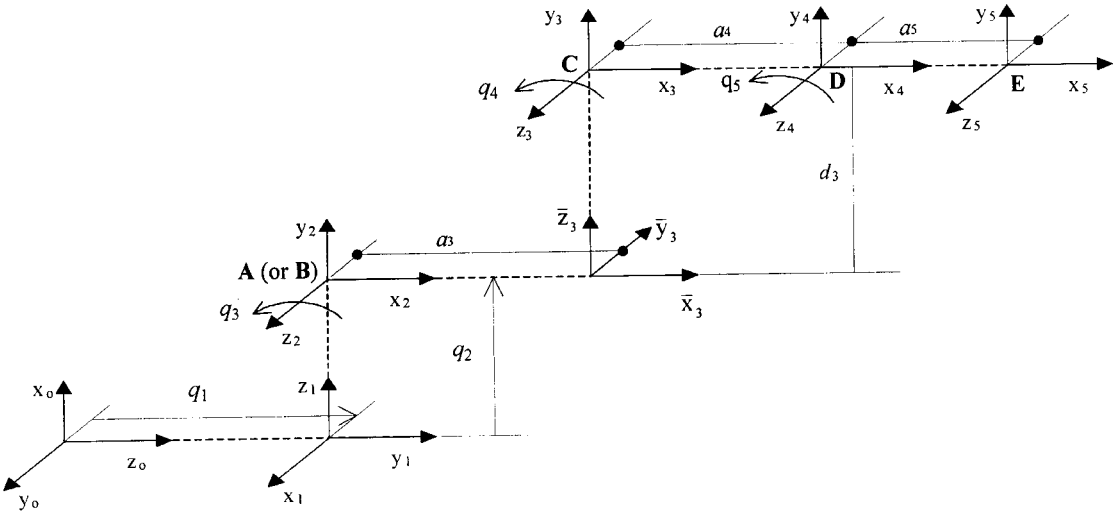

Fig. 3. Link coordinate systems pertaining to Figure 2.

https://doi.org/10.1017/S0263574702004423 Published online by Cambridge University Press

where **g** is the gravitational acceleration vector in base coordinate frame, $\mathbf{r}_i^i$ is the position vector of mass center of link i in coordinate frame i. In Equations (4), (5), and (6), $\mathbf{T}_i$ is the homogeneous transformation matrix from coordinate frame i to the base coordinate frame. $\mathbf{J}_i$ is defined as:

$$\mathbf{J}_i = \begin{bmatrix} \mathbf{J}_i^i + m_i \mathbf{r}_i^i \mathbf{r}_i^{iT} & m_i \mathbf{r}_i^i \\ m_i \mathbf{r}_i^{iT} & m_i \end{bmatrix}$$

where $\mathbf{J}_i^i$ is a 3×3 inertial matrix of link i about its mass center in coordinate frame i and m_i is the mass of link i. Δ_i is a differential operator; it is defined as:[20]

$$\Delta_i = \begin{bmatrix} \lambda_i \tilde{\mathbf{z}}_{i-1} & [\lambda_i \tilde{\mathbf{p}}_{i-1} + (1-\lambda_i)\mathbf{I}]\, \mathbf{z}_{i-1} \\ 0 & 0 \end{bmatrix} \qquad (7)$$

where $\mathbf{z}_i$ is z-*axis* of coordinate frame i, and $\mathbf{p}_i$ is the position vector of the origin of coordinate frame i with respect to the base coordinate. $\lambda_i = 1$ for revolute joints; $\lambda_i = 0$ for prismatic joints. **I** is the identity matrix. The symbol '~' in (7) denotes a skew symmetric matrix with zero diagonal values. For example, given a vector $\mathbf{u} = \{u_x, u_y, u_z\}^T$, $\tilde{\mathbf{u}}$ is defined as:

$$\tilde{\mathbf{u}} = \begin{bmatrix} 0 & -u_z & u_y \\ u_z & 0 & -u_x \\ -u_y & u_x & 0 \end{bmatrix}$$

The elements of the external forces due to the suspension are derived from general equation,

$$\tau_{susp_i} = \frac{\partial R}{\partial \dot{q}_i} + \frac{\partial V_{sp}}{\partial q_i},$$

where R is Rayleigh's dissipation function and V_{sp} is potential energy function due to the springs.

For phase 1, we have (refer to Fig. 2a):

$$R = \frac{1}{2}[B_1 \dot{q}_2^2 + B_2(\dot{q}_2 + l_3 \dot{q}_3)^2]$$

and

$$V_{sp} = \frac{1}{2}[k_1(q_2 - x_0)^2 + k_2(q_2 + l_3 q_3 - x_0)^2]$$

Thus

$$\tau_{susp} = \{0, F_{susp1} + F_{susp2}, -l_3 F_{susp2}, 0, 0\}^T$$

For phase 2, we have (refer to Fig. 2b):

$$R = \frac{1}{2}[B_2 \dot{q}_2^2 + B_1(\dot{q}_2 - l_3 \dot{q}_3)^2]$$

and

$$V_{sp} = \frac{1}{2}[k_2(q_2 - x_0)^2 + k_1(q_2 - l_3 q_3 - x_0)^2]$$

$$\tau_{susp} = \{0, F_{susp1} + F_{susp2}, l_3 F_{susp1}, 0, 0\}^T$$

In the above equations, B_1, B_2 are the damping coefficients, k_1, k_2 are the spring constants, l_3 is the distance between the front and rear edges, and x_0 is the natural (undeformed) length of the springs.

4. SIMULATION RESULTS

In this section, the developed model is applied to a Caterpillar log-loader as shown in Figure 4. The machine is a mobile three-degree of freedom manipulator with an additional moveable implement. The implement is a grapple for holding and handling objects such as trees. The whole machine can move forward or backward. The upper structure of the machine rotates on the carriage by a 'swing' hydraulic motor through a gear train. 'Boom' and 'stick' are the two other links, which together with the 'swing', serve to position the implement. Boom and stick are operated through hydraulic cylinders. The cylinders and the swing motor are activated by means of pressure and flow through the main valves. Modulation of the oil flow in the main valves is presently controlled by the pilot oil pressure through manually operated pilot control valves. The

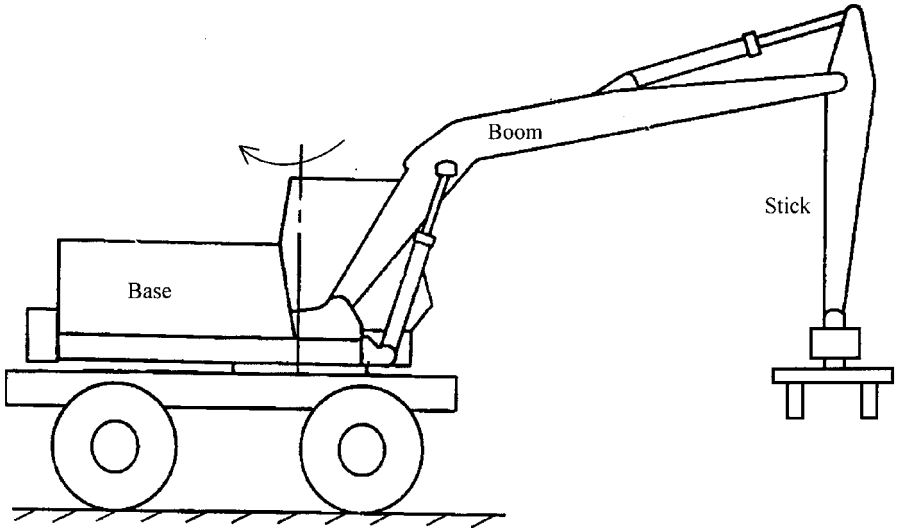

Fig. 4. Typical Caterpillar excavator-based log-loader.

https://doi.org/10.1017/S0263574702004423 Published online by Cambridge University Press

Table I. Kinetic parameters of Caterpillar log-loader.

Link	θ_i	d_i	a_i	α_i	Variables
1	$\pi/2$	q_1	0	$\pi/2$	q_1
2	$\pi/2$	q_2	0	$\pi/2$	q_2
3	q_3	0	$a_3 = 4\ m$ (or $-1\ m$)	$-\pi/2$	q_3
3	0	$d_3 = 1.5$ m	0	$\pi/2$	–
4	q_4	0	$a_4 = 5.2$ m	0	q_4
5	q_5	0	$a_5 = 1.8$ m	0	q_5

Table II. Dynamic parameters of Caterpillar log-loader.

	mass (kg)	mass moment of inertia (kg m^2)	Center of gravity (x, y, z) m	Coordinate frame (refer to Figure 3)
Base	12,000	90,523	(–2.0, –0.6, 0.0)	$\{x_3y_3z_3\}$
Boom	1,830	15,500	(–2.9, 0.2, 0.0)	$\{x_4y_4z_4\}$
Stick	688	610	(–0.9, 0.1, 0.0)	$\{x_5y_5z_5\}$

equations governing the hydraulic actuation system are given in details in reference [1] and thus are not repeated here.

Here, the swing is locked. Thus, the movement of the implement is limited to a planar motion. Also, it is assumed that the friction between the base and the ground is enough to allow the base to only rotate around the front or the rear edges and to prevent the machine from moving forward or backward. The kinematic and dynamic parameters of the machine are given in Tables I and II respectively. The suspension parameters are chosen as $k_1 = k_2 = 35 \times 10^5\ N/m$ and $B_1 = B_2 = 15 \times 10^4\ Ns/m$. These values provide a static deflection of approximately 4 cm (chosen arbitrarily) with a response slightly below critical damped.

The simulated task is to have the machine end-effector to perform a pick and place operation. In this task, the end-effector starts from a position close to the base carrying 5000 kg load. The base is initially stable. The manipulator extends the end-effector to a possible 'dumping position' far from the base. Figure 5 shows the corresponding link motions.

With reference to Figure 6a, this move causes the machine to tip-over when the end-effector extends its arm far enough from the base. Figure 6b shows the movement of the front edge during the task. After the base rotates about 8 degrees (clockwise) over the front edge, the implement retracts back to regain the stability. As is seen, the machine starts to roll back to a stable position. Note that, at time $t \cong 5$ seconds, at which the implement starts moving, the base experiences a slight pitch motion. This is due to the coupled dynamics between the base and the other links.

The effects of various suspension stiffness and damping, on the stability, are also studied. The responses are compared with that obtained using the previous model by the authors in which no suspension was included.[1] Figures 7 and 8 show the results of using different stiffness and damping coefficients, respectively. Figure 7 clearly shows that the stability of the system decreases as the flexibility of the suspension increases. On the other hand, Figure 8 indicates that the stability of the system decreases by decreasing the damping. It is also seen that

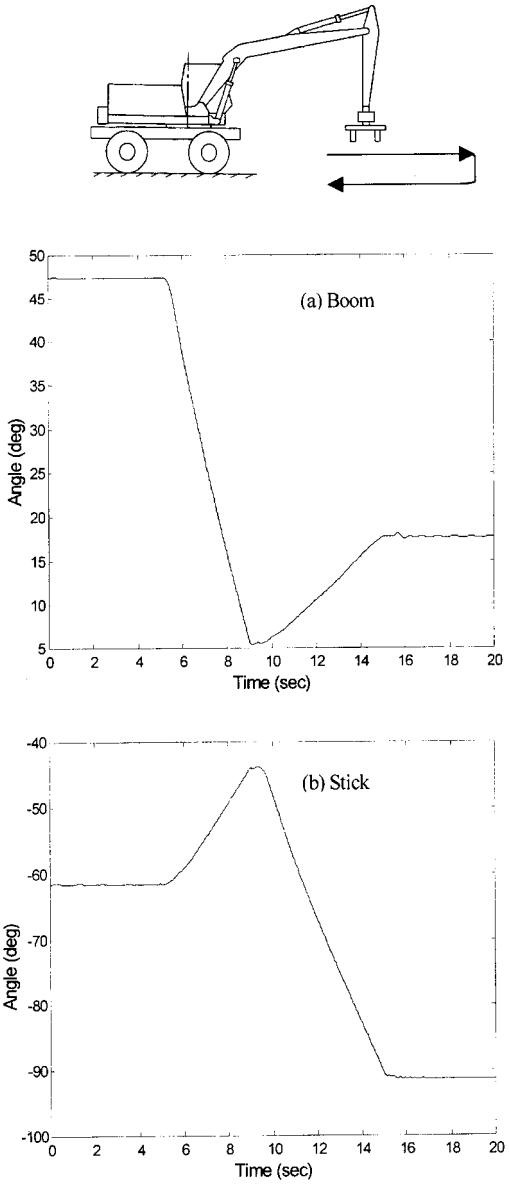

Fig. 5. Manipulator movement during a pick and place operation.

https://doi.org/10.1017/S0263574702004423 Published online by Cambridge University Press

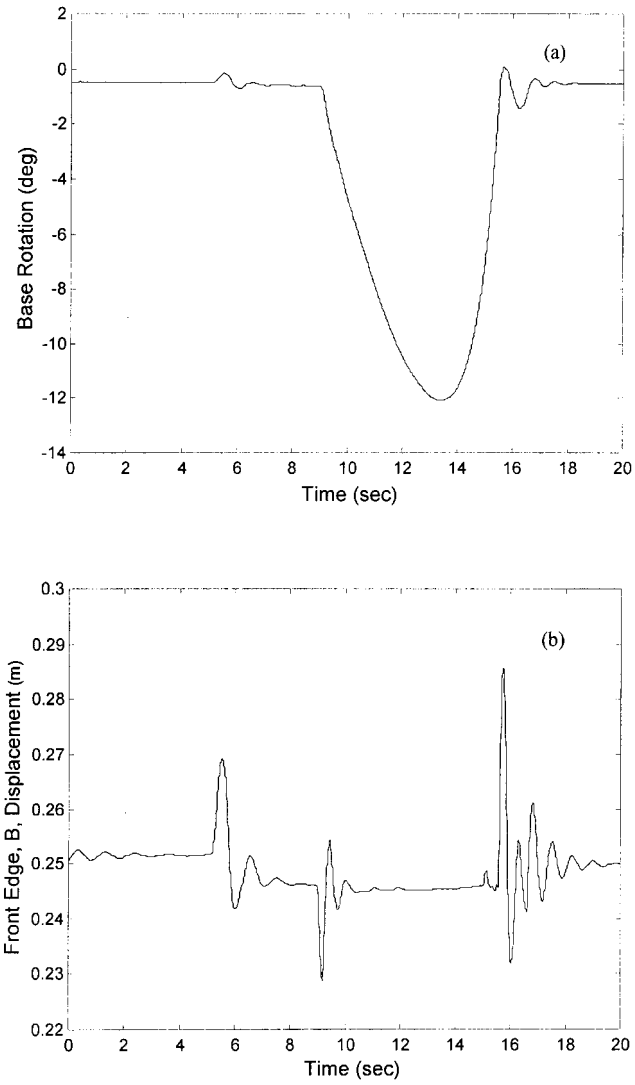

Fig. 6. History of: (a) base rotation and (b) front edge movement, during the task.

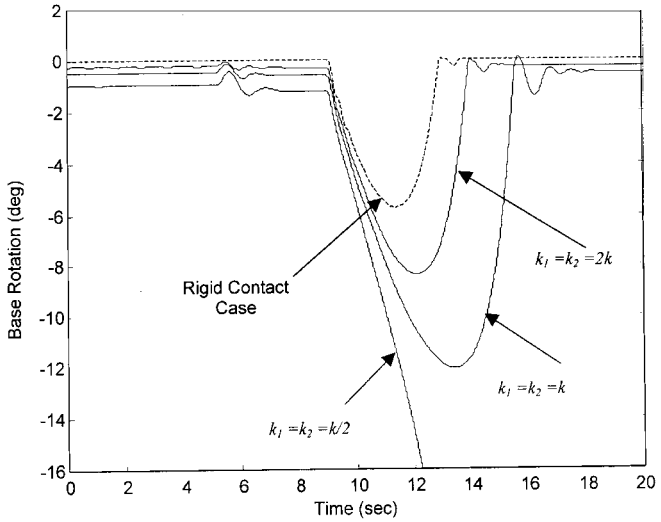

Fig. 7. Effect of increasing the suspension stiffness while the damping coefficient is kept constant, $k = 35 \times 10^5$ *N/m* and $B_1 = B_2 = 15 \times 10^4$ *Ns/m*.

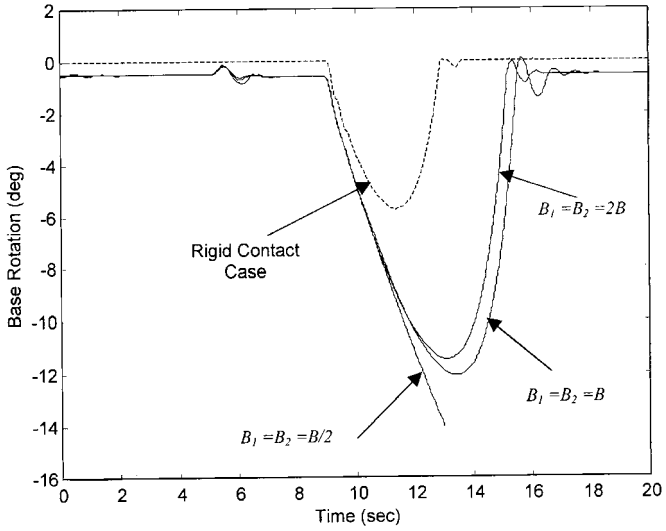

Fig. 8. Effect of increasing the suspension stiffness while the damping coefficient is kept constant, $k = k_2 = 35 \times 10^5$ *N/m* and $B_1 = B_2 = 15 \times 10^4$ *Ns/m*.

changing the system stiffness has a greater influence on the stability of the machine than that of the system damping. Overall, the angular movement of the base during the whole manipulator motion, in the case of flexible contact, is greater than the angular movement of the base for the rigid contact case. This indicates that the compliance between the base of the manipulator and the ground tends to reduce the machine stability.

5. CONCLUSIONS

In this paper, a dynamic model for a two-link planar mobile manipulator was developed. The model takes into account both the detailed dynamics of the base that can rock back-and-forth during the movement of the manipulator and the flexibility between the base and the ground. Sirnulation results were presented to substantiate the model development presented here. In particular, the trend of the results was found to be consistent with the ones from the model that previously developed by the authors in which rigid contact was assumed between the base and the ground. However, it was shown that the flexibility of the contact reduces the manipulator's stability. Therefore, the flexibility between the base and the ground should be considered in the dynamic model to accurately investigate the stability of mobile manipulators. The proposed model therefore, provides simulation capabilities towards the stability analysis of manipulators mounted on mobile platforms. It also facilitates design of suitable tipover prevention schemes. This is significant, since with the introduction of computer control, safety, productivity and lifetime of mobile manipulators could be improved by automatic prediction, prevention and recovering from tip-over.

REFERENCES

1. R.F. Abo-Shanab and N. Sepehri, "On Dynamic Stability of Manipulators Mounted on Mobile Platforms," *Robotica* **19**, 439–449 (2001).
2. N. Sepehri, P. D. Lawrence, F. Sassani and R. Frenette, "Resolved mode teleoperated control of Heavy Duty

https://doi.org/10.1017/S0263574702004423 Published online by Cambridge University Press

Hydraulic Machines," *ASME Journal of Dynamic Systems, Measurement, and Control* **116**, 232–240 (1994).
3. N. Sepehri and P. D. Lawrence, "Mechatronic System Techniques in Teleoperated Control of Heavy-Duty Hydraulic Machines." In: *Mechantronic Systems Techniques and Applications* (editor: C. T. Leondes) Gordon and Breach Science Publishers, Amsterdam, Netherlands, (2000) **Vol. 3**, 309–373.
4. D. Messuri and C. Klein, "Automatic Body Regulation for Maintaining Stability of a Legged Vehicle During Rough-Terrain Locomotion," *IEEE Journal of Robotics and Automation*, RA-1 No. 3, 132–141 (1985).
5. P. V. Nagy, S. Desa, and W. L. Whittaker, "Energy-Based Stability Measure for Reliable Locomotion of Statically Stable Walkers: Theory and Application," *Int. J. Robotics Research* **13**, No. 9, 272–287 (1994).
6. S. Dubowsky and E. E. Vance, "Planning Mobile Manipulator Motions Considering Vehicle Dynamic Stability Constraints," *Proc. IEEE Int. Conf. on Robotics and Automation* **Vol. 3** (1989), 1271–1276, Scottsdale.
7. S. Sugano, Q. Huang and I. Kato, "Stability Criteria in Controlling Mobile Robotic Systems," *Proc. IEEE/RSJ Int. Conf. on Intelligent Robots and Systems*, Yokohama, Japan (1993) **Vol. 3**, pp. 832–838.
8. Q. Huang and S. Sugano, "Manipulator Motion Planning for Stabilizing a Mobile Manipulator," *Proc. IEE Int. Conf. on Intelligent Robots*, Pittsburg, PA (1995), pp. 467–472.
9. Q. Huang, S. Sugano and K. Tanie, "Motion Planning for a Mobile Manipulator Considering Stability and Task Constraints," *Proc. IEEE Int. Conf. on Robotics and Automation*, Leuvan, Belgium (1998) **Vol. 3**, pp. 2192–2198.
10. Q. Huang, S. Sugano and K. Tanie, "Stability Compensation of a mobile Manipulator by Manipulator Motion: Feasibility and Planning," *Proc. IEEE/RSJ Int. Conf. on Intelligent Robots and Systems* (1997), pp. 1285–1292.
11. E. G. Papadopoulos and D. A. Rey, "A New Measure of Tipover Stability Margin for Mobile Manipulators," *Proc. IEEE Int. Conf. on Robotics and Automation*, Minneapolis, Minnesota (1996), pp. 3111–3116.
12. E. G. Papadopoulos and D. A. Rey, "The Force-Angle Measure of Tipover Stability Margin for Mobile Manipulators," *Journal of Vehicle System Dynamics* **33**, 29–48 (2000).
13. K. Iagnemma, A. Rzepniewski, S. Dubowsky, P. Pirjanian, T. Huntsberger, P. Schenker, "Mobile Robot Kinematic Reconfigurability for Rough-Terrain," *Proc. SPIE's Int. Symposium on Intelligent Systems and Advanced Manufacturing*, Boston, MA (2000), Paper No. 4196–47.
14. A. Ghasempoor and N. Sepehri, "A Measure of Stability for Mobile Manipulators With Application to Heavy Duty Hydraulic Machines," *ASME Journal of Dynamic Systems, Measurement, and Control* **120**, 360–370 (1998).
15. Q. Wu, S. Onysho, N. Sepehri, and A. B. Thronton-Trump, "On Construction of Smooth Lyapunov Functions for Non-Smooth Systems," *Int. J. of Control* **69**, 443–457 (1998).
16. A. F. Filippov, Differential Equations with Discontinuous Right-Hand Side, *Math. Sbornik* **51**, 99–128 (1960). (English translation: *American Mathematical Society Translations* **42**, 199–231, (1964)).
17. A. F. Filippov, "Differential Equations with Second Members Discontinuous on Intersecting Surfaces," *Differentsial'nye Uravneniya* **15**, 1814–1832 (1977). (English translation: *Differential Equation* **15**, 1292–1299, (1980)).
18. K. S. Fu, R. C. Gonzalezand C. S. G. Lee, *Robotics: Control, Sensing, Vision, and Intelligence* (McGrawHill, Singapore, 1987).
19. M. M. Sallam, R. F. Abo-Shanab and A. A. Nasser, "Modified Methods for Dynamic Modeling of Robot Manipulators," *Proc. ASME Engineering Technical Conf.* Atlanta, GA (1985), Paper No. DETC98/MECH-5860 (1995).
20. R. F. Abo-Shanab, N. Sepehri and Q. Wu, "On Dynamic Modelling of Robot Manipulators: The Method of Virtual Links," to be presented at *ASME Design Engineering Technical Conference* Montreal, Canada (Sept. 29 – Oct. 2, 2002).
21. U. O. Akpan and M. R. Kujath, "Sensitivity of a Mobile Manipulator, Response to System Parameters," *ASME Journal of Vibration and Acoustics* **120**, 156–163 (1998).

https://doi.org/10.1017/S0263574702004423 Published online by Cambridge University Press